Journal of Applied and Natural Science
17(4), 1674 - 1685 (2025)
ISSN : 0974-9411 (Print), 2231-5209 (Online)
journals.ansfoundation.org

Research Article

Adsorption capacity study of isolated cellulose and its nanocomposite for Safranine T dye in aqueous solutions

Hawraa Kadhim Abdul-hussein
Department of Ecology, College of Science, University of Basrah, Basrah, Iraq
Munther Abduljaleel Muhammad-Ali*
Department of Ecology, College of Science, University of Basrah, Basrah, Iraq

*Corresponding author: E-mail: munther.ali@uobasrah.edu.iq

Article Info
https://doi.org/10.31018/jans.v17i4.6944
Received: July 05, 2025
Revised: November 04, 2025
Accepted: November 15, 2025

How to Cite

Abdul-hussein, H. K. and Muhammad-Ali, M. A. (2025). Adsorption capacity study of isolated cellulose and its nanocomposite for Safranine T dye in aqueous solutions. *Journal of Applied and Natural Science*, 17(4), 1674 - 1685. https://doi.org/10.31018/jans.v17i4.6944

Abstract

Synthetic dyes are widely used in textiles, paper, plastic, and other industries, which are toxic and harmful to the environment and humans. Adsorption is an efficient method to control wastewater. Cellulose is an abundant, renewable, and eco-friendly polymer produced by plants and trees. This study examined the possibility of using extracted free cellulose from corrugated cardboard (CC), cellulose composite with AgNPs of *Myrtus communis* L. extract (CAgM) and cellulose composite with AgNPs of banana peel extract (CAgB) for the removal of the cationic dyes, Safranine-T (ST), from aqueous solutions. The scope of this research included the characterization of sorbents using Fourier Transform Infrared Spectroscopy (FTIR), Scanning Electron Microscope (SEM), Energy Dispersive X-ray Spectroscopy (EDX), X-Ray Diffraction (XRD), Gas Chromatography–Mass Spectrometry (GC-MS), Ultraviolet–Visible Spectroscopy, determination of time contact, adsorbent mass, pH and temperature effect on the effectiveness of dye sorption using 50 mL of solution. The use of waste paper materials as sorbents was found not to pose any severe risk of aquatic environment contamination. Safranine-T (ST) sorption intensities were the highest at pH 8 and pH 10. The waste paper sorbents proved particularly effective in removing cationic dyes, like in the case of CC and CAgM, which had a sorption capacity that reached 89.16% and 84.22 %, respectively, and 84.04% towards CAgM. An adsorption isotherm study showed that the best equation used to describe the adsorption system is the Freundlich equation, with excellent correlation $R^2 > 0.9707$.

Keywords: Adsorption isotherm, banana peel , Cellulose, Corrugated cardboard, Silver nanoparticle, Safranine-t dye

INTRODUCTION

Water is paramount and important for the sustainable development of a healthy life throughout the world. However, water pollution with numerous industrial noxious elements is recently considered as the greatest stimulating substance throughout the world, particularly in developing countries (Islam *et al.,* 2018a). Nowadays, the presence of various contaminants, including toxic inorganic nutrients, different organic species, and fuel-related products, have been reported throughout the world in aquatic systems (Padilla *et al.,* 2017). As a result of their noxiousness and bioaccumulation, the pollutants stated above pose prodigious hazards for individuals and other environments. The growth in the global population and expansion has put more pressure on the industry. Textile businesses in several nations struggle to meet human demands (Baig *et al.,* 2019). These industrial operations consume large amounts of water and produce massive amounts of wastewater containing organic and inorganic compounds such as dyes. Currently, 95-400 L of water is consumed for every kilogram of fabric manufacture. In general, dyes are more soluble and can easily discharge effluents into the environment, posing substantial environmental risks (Islam *et al.,* 2018b).

Safranine-T (ST) is a synthetic cationic dye with the chemical formula $C_{20}H_{19}ClN_4$ (3,7-dimethyl-10-phenylphenazin-10-ium-2,8-diaminechloride) that can be found as powder or reddish crystals. This dye is widely used in dyeing cotton, silk, tannin, wool, leather, bast fibers, and paper, and it is regarded as a model compound for the dyes emitted into textile industry effluents (Ritter *et al.,* 2024). Cationic dyes represent a larger danger than anionic dyes because of their easy and powerful contact with negatively charged cell membranes, which can induce allergies and respiratory

problems (Saha *et al.,* 2021). Dye contamination, particularly with Safranine-T, can induce stomach discomfort, respiratory tract irritation, throat discomfort, and irritation and redness of the eyes and skin. Environmental protection agencies and legislation require compliance with acceptable limits for dye discharge in wastewater, which must be eliminated before release into streams (Suleman *et al.,* 2021).

Toxic contaminants are eliminated using a variety of processes, including adsorption, coagulation, precipitation, filtering, solvent extraction, reverse osmosis, and ion exchange. Adsorption is the most cost-effective and efficient method for eradicating contaminants, with a wide range of sorbent resources available, including carbon-activated materials and nanotubes (Bayuo *et al*., 2021). Natural-based resources (cellulose, chitin, chitosan, gelatine, and others) are now chosen for the eradication of toxic dyes from water due to their low cost and ease of reuse. From these polymeric materials, cellulose gains the advantages of being comparable, easily accessible, non-toxic, and rich in hydroxyl functional groups that can be used in many chemical modification operations (Kara *et al.,* 2021).

Despite their distinguishing characteristics, the disadvantages of cellulose-based materials in contaminated water cleaning include delayed hydrophilicity, lower physical and chemical stability, and reduced pollutant uptake competence. As a result, the production of nanomaterials for adsorbing adsorbates is becoming more prevalent (Ahankari *et al.,* 2020). In this approach, reactive hydroxyl and carboxyl groups from natural bio-derived materials were used as environmentally benign reducing agents, replacing harmful reductive organic species such as sodium borohydride ($NaBH_4$), hydrazine, and dimethylformamide (DMF), which pose potential environmental and biological risks (Dhaka *et al.,* 2023). Cellulose, an abundant natural polymer, is used as an ideal green reducing agent candidate because of its mild reductive activity, which is caused by a large number of hydroxyl and ether groups on its polysaccharide chains (Mishra *et al.,* 2024).

Sedighi *et al.* (2014) employed heat energy to enhance the reduction power of cotton fabric in the manufacture of copper and copper oxide nanoparticles. Fernandez *et al.* (2010) created a silver nanocomposite with cellulose nanofibers using heat and UV radiation. Nadagouda and Varma (2007) and Chen *et al.* (2007) used microwave-assisted green synthesis to create transition metal nanoparticles (copper, silver, indium, and iron) by using carboxymethyl cellulose sodium as a reducing and stabilizing reagent. The direct production or growth of metal nanoparticles on cellulosic materials has several uses, including fabrics and textiles, catalysis, biomedical devices, and active packaging (Abu-Elghait *et al.*, 2021).

Safranine-T is comparatively understudied because the majority of adsorption research has concentrated on dyes like Methylene Blue and Crystal Violet. Furthermore, there are currently few studies comparing isolated cellulose and its nanocomposites under various parameters (temperature, pH, and starting concentration). The present study examined the possibility of using the corrugated cardboard (CC) and its AgNPs composites as unconventional sorbents for removing cationic dye Safranine-T (ST) from aqueous solutions. The scope of research included the determination of solution pH on the effectiveness of dye sorption, sorption kinetics, and the maximum sorption capacity of the tested sorbents.

MATERIALS AND METHODS

Materials and instruments

Materials used include silver nitrate $AgNO_3$ (99.92%, Sigma), Philippian banana peel *Musa acuminata* (local market), Common Myrtle *Myrtus communis* L. (Home garden), old corrugated cardboard (OCC, local market), 4% NaClO and Safranine-T dye (Merck), HCl (36%, HiMedia, India), NaOH (99.9%, HiMedia, India), pH meter (China), Incubator Shaker (Model Innova 42, New Brunswick Scientific, Canada), Hot plate with magnetic stirrer (China) , Centrifuge (Model PLC-012, Gemmy Instrument Corp., Taiwan), UV-Visible Spectrophotometer.

Preparation of the aqueous extract of banana peels and *Myrtus communis L.*

Banana peels and *Myrtus communis* L. were separately washed with distilled water to provide an aqueous extract. Ten grams of finely chopped peels and *Myrtus communis* L. separately were combined with 100 ml of distilled water and gently heated (about 50 ^{o}C) with continuous magnetic stirring for 30 min. The extract was filtered and the extract was preserved in the refrigerator at 4°C until use. (Alasadi *et al.*, 2024; Štular *et al.*, 2021)

Biosynthesis of silver nanoparticles (AgNPs) (Green Synthesis)

The concentration of 2 mM of $AgNO_3$ solution was prepared by dissolving 0.03g in 100 mL of deionized distilled water. This solution was mixed with 25 mL of aqueous banana peel or *Myrtus communis* L. extracts, heated gently, and stored overnight in the dark. The color was changed to dark brown, indicating the formation of silver nanoparticles. The resulting mixture was harvested by centrifuging and redispersing the precipitate in distilled water to obtain purified particles. The samples were oven-dried for further characterization (Daish *et al.*, 2024; Tomar *et al.*, 2017).

Characterization of silver nanoparticles (AgNPs)

UV-Vis spectroscopy, a powerful analytical instrument, was employed to characterize the greenly synthesized AgNPs and validate the reduction procedure for AgNPs

synthesis. Fourier transform infrared spectroscopy was performed with a Thermo Scientific Nicolet 6700 FT-IR spectrometer (Waltham, MA, USA) to detect the presence of potential biomolecules and functional groups. The structure of the silver nanoparticles was analyzed by X-ray diffraction (Rigaku Ultima IV, Neu-Isenburg, Germany XRD). Crystallite domain size was determined using D. Scherrer's equation. The form and size of phytomediated AgNPs were imaged using transmission electron microscopy (TEM; JEM-1011; JEOL Ltd., Tokyo, Japan).

Cellulose extraction

Preparing an old corrugated cardboard (CC) sample

A sample of 25 g of old CC was weighed and divided into smaller pieces. It was then immersed in water for 24 hours. CC was filtered through a muslin cloth and rinsed completely with distilled water. After air-drying, it was stored in a polyethylene bag until ready for use.

Extraction of cellulose from corrugated cardboard (**CC)**

Alkaline treatment

CC was treated with 4% NaOH at 100□ for 2 hr with mechanical stirring; this treatment was repeated twice to generate a suspension. Then it was filtered and rinsed with distilled water until the pH was neutral (Rasli, 2017).

Bleaching treatment

The CC sample was bleached with 4% NaClO and agitated mechanically for 3 hr at 100□ (Walawska *et al.*, 2024). Bleaching treatment steps were repeated twice, similar to the alkaline treatment, for improved extraction. Following each treatment, the CC suspension was filtered and rinsed with distilled water until it reached neutral pH, then left to dry.

Preparation of a cellulose-silver nanocomposite

A cellulose-silver nanocomposite was prepared by mixing 100 ml of a previously prepared AgNPs solution of *Myrtus communis* L. (AgM) or banana peels (AgB), with 10 g of the prepared cellulose (CC) in 100 ml of solution and stirring continuously for 2 hr to give cellulose composite with AgNPs of *Myrtus communis* L. extract (CAgM) and cellulose composite with AgNPs of banana peel extract (CAgB), respectively. The suspension was filtered and dried at 50°C (Ahmad *et al.,* 2013).

Adsorption studies

Batch adsorption tests were conducted in 100 mL flasks with 50 mL of working volume, using 100 mg L^{-1} of Safranine-T dye due to its chemical or physical properties, availability, and ease of handling. A weighed amount of adsorbent (0.2, 0.4, and 0.6 g) was added to the solution. The flasks were agitated at a constant speed of 120 rpm for 24 hr in an incubator shaker at 25° C. The present study examined the adsorbent mass (0.2, 0.4, 0.6 g), contact duration (0.25, 0.5, 1, 2, 3, 4,5, and 24 hr), and at fixed temperature (25° C) were assessed during the current investigation. After equilibrium, the solution was centrifuged at 4000 rpm for 10 min, then measured using a UV-VIS spectrophotometer at 460 nm for SF. The adsorption efficiency (R%) and mass balance were used to calculate the amount of dye adsorbed per unit adsorbent. Loading capacity (mg dye per g adsorbent) during data processing was calculated using Eq. (1):

$$R\% = \left(\frac{C_o - C_t}{C_o}\right) x\ 100 \quad (1)$$

$$q_e = \frac{(C_0 - Ce)v}{m} \quad (2)$$

Using equations (1) and (2), the removal efficiency (R) and equilibrium adsorption capacities (qe) were computed. Where m is the mass of the adsorbent (g), V is the volume of the solution (L), and C_o and C_e are the starting and equilibrium concentrations of SF (mg L^{-1}), respectively.

At constant time contact of 2 hr and 0.4 g of adsorbent concentration, pH and temperature effects were studied at 2, 4, 6, 8, and 10, and 25, 35, and 45 °C, respectively. Removal efficiency (R) and equilibrium adsorption capacities (qe) were calculated using equations (1) and (2), respectively.

Adsorption isotherms

The interaction between the adsorbent and the adsorbate is described by the adsorption isotherm, which is essential for maximizing the adsorbent's utilization. The most suitable correlation for the equilibrium curve must be determined in order to optimize the design of an adsorption system to remove contaminants from liquids. Cellulose's adsorption equilibrium data for SF were used to create the Freundlich, Langmuir, and Temkin adsorption isotherms in this investigation. Parameters Ce and qe were correlated using these three types of equations at three temperature degrees, 25, 35, and 45 °C.

Statistical analysis

In SPSS v. 20 for Windows, two-way ANOVA was used for statistical analysis, and Duncan's new multiple range test (≤ 0.05) was used to determine the mean separation between treatments.

RESULTS AND DISCUSSION

Gas chromatography–mass spectrometry (GC-MS) results

The results of gas chromatography-mass spectrometry showed the presence of various types of aromatic and aliphatic compounds. Table 1 and Fig. 1 indicate the components of the aqueous extract of banana peels, which revealed that there are compounds with high

concentrations belonging to the organic categories of alcohols, phenols, carboxylic acids, and non-homogeneous cyclic compounds, with concentration ratios ranging from 14.69% to 1.03%. Table 2 and Fig. 2 represent the plant components of the aqueous extract of the plant *Myrtus communis L.*, where the presence of active compounds such as alcohols, phenols, non-homogeneous cyclic compounds, and amides (Jasim *et al.*, 2024) is also noted, with concentration ratios ranging from 30.45% to 1.06%.

Fourier transform infrared spectroscopy (FT-IR) spectrum

Cellulose (CC) showed characteristic bands at 3279.06, 2924.62,1414.73, and 1024.46 cm^{-1}, related to O-H stretching, CH_2 stretching, C-H bending, C-O-C pyranose ring vibration, and β-glycosidic linkage between the glucose units in cellulose, respectively (Salman *et al.*, 2020). The peaks located at 1634.13 cm^{-1} correspond to the vibration of water molecules absorbed in cellulose. Cellulose-Ag with banana peels (CAgB) showed the same cellulose peaks with some other peaks 1688.80, 1650.98, 1424.02, 1320.04, 1099.89, and 664.94 cm^{-1}, which are attributed to aromatic compounds adsorbed on silver particles. Cellulose-Ag with *Myrtus communis* extract (CAgM) gave the same cellulose peaks, which may be attributed to low loading of silver to cellulose (Fig. 3).

Characterization of AgNPs nanoparticles

UV-Visible spectrum (UV-VIS)

In the current study, we generated stable silver nanoparticles utilizing the bioreduction method with biowaste from banana peel and *Myrtus communis* L. inde-

Table 1. Plant components of the aqueous extract of banana peels

Peak	R.T.	Area Pct	Library/ID	Chemical Structure
27	13.113	14.6923	4H-Pyran-4-one, 2,3-dihydro-3,5-dihydroxy-6-methyl-	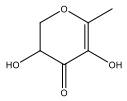
32	13.906	11.1541	Catechol	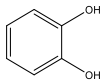
35	14.37	8.5091	5-Hydroxymethylfurfural	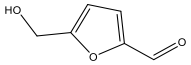
38	15.037	7.0078	Hydroquinone	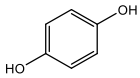
36	14.755	3.4192	1,2-Benzenediol, 3-methyl-	
44	16.561	2.6517	1,2,3-Benzenetriol	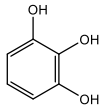
21	11.919	2.1321	Methyl 2-furoate	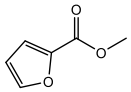
20	11.738	2.1282	Furaneol	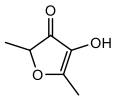
43	16.381	1.8522	Chloroxylenol	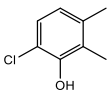
14	9.067	1.7471	2-Cyclopenten-1-one, 2-hydroxy-	
62	24.417	1.6585	Oleic Acid	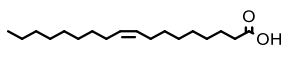
37	14.927	1.0369	1-(2,3-Dihydroxyphenyl)ethanone	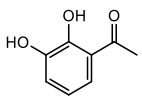

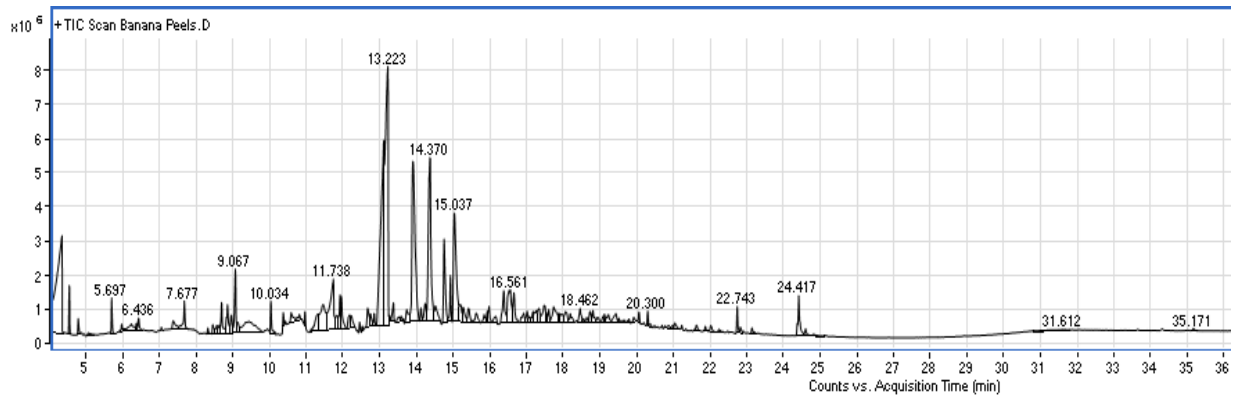

Fig. 1. *Gas chromatography-mass spectroscopy (GC-MS) chromatogram of the aqueous extract of banana peels*

pendently. To validate the synthesis of silver nanoparticles, UV-VIS spectral scanning was performed at wavelengths ranging from 350 to 700nm. The color change of silver nitrate solution was seen at various time intervals, namely 1 hour, 2 hours, 4 hours, and 24 hours, and spectra were recorded, with a sharp peak observed at 430 nm wavelength for banana peel and 420 nm for *Myrtus communis L*. (Fig. 4). The color change indicates that Ag (I) has been transformed into Ag(0), as the intensity increases with reaction time. The extracts' phytochemicals are essential to the environmentally friendly production of silver nanoparticles. Silver ions (Ag□) can be reduced to metallic silver (Agº) by phenolic substances and flavonoids, donating electrons to them through their hydroxyl and carbonyl groups.

X-ray Diffraction analysis (XRD)

Using the Debye-Scherrer equation and the AgNPs crystal size rate recorded at the 100% peak, the X-ray diffraction spectrometer demonstrated the size and crystal nature of AgNPs. The crystal volume rate was 45.10nm for *Myrtus communis L.*, and the crystal nature of AgNPs. The crystal volume rate was 18.56 nm for banana peel (Fig. 5).

Scanning electron microscopy (SEM) analysis

The generated AgNPs were spherical in shape and had a narrow size range, 33.56 and 69.71 nm, for AgNPs of banana bells and *Myrtus communis* L., respectively, as shown in Fig. 6A and 6B. EDX patterns of cellulose composites gave different percentages of elements, which were attributed to Ag, C, and O. Fig. 7A showed the presence of these elements with percentages 3.87, 42.46, and 39.90%, whereas Fig. 7B gave 5.01, 44.00, and 41.00% for Ag, C, and O, respectively. These percentages enhanced the presence of Ag metal in cellulose materials (Alfarraj *et al.*, 2023)

Dye removal

Effect of contact time

The removal of safranine dye was conducted on the effect of contact time treated with materials (CC, CAgB, and CAgM) for a period of 0.25, 0.5, 1, 2, 3, 4, 5, and 24 hr. It is noted that there is a proportional relationship between time and R% and q_e with time, and the best time is after 24 hr. It can be inferred that the removal of dye using CC gave maximum efficiency R% = 84.73 as compared with CAgM and CAgB, (R%, 82.28 and 73.88, respectively), as shown in Fig. 8. In same manner, CC gave the maximum adsorption capacity (qe), and the rank of capacity (CC; 21.17 > CAgM; 20.55 > CAgB; 18.46 mg/g), as shown in Fig. 9. The results of the statistical analysis indicated significant differences between cellulose types and the time contact at ≤0.05.

Effect of initial pH of the solution

The pH of the dye solution is an important parameter in the adsorption process. The results of this study are presented graphically in the Figs. 10 and 11. The removal of safranin dye was conducted based on the pH effect treated with the materials (CC, CAgB, and CAgM) at pH levels (2, 4, 6, 8, 10). It is concluded that the best pH for dye removal is 8, using CC and CAgM, which gave a maximum efficiency (R%, 89.16 and 84.22, respectively), and that the best pH for dye removal is 10 using the CAgB material gave a maximum efficiency R% = 84.04. The biosorption of SF on the biosorbent's surface is affected by the biosorbent's surface charge and the solution's initial pH. The results of the statistical analysis indicated significant differences between types of cellulose used and the pH at ≤0.05. This interaction highlights the importance of optimizing pH levels to enhance dye removal efficiency.

Effect of temperature

The three temperatures at which the experiments were conducted were 25, 35, and 45 ◦C (Figs. 12 and 13). The percentage of dye for safranine dropped from 89.16% to 83.01% for CC and from 84.04% to 82.89% for CAgB, and from 84.22 % to 83.31 % for CAgM as the temperature rose. This pattern suggests that the process of adsorption was exothermic. Jóźwiak *et al.* (2024) suggest that this could be due to a rise in the rate at which dye molecules diffuse through the sorbent's internal pores and external boundary layer,

Table 2. The plant components of the aqueous extract of *Myrtus communis L.*

Peak	R.T.	Area Pct	Library/ID	Chemical Structure
19	14.456	30.4566	5-Hydroxymethylfurfural	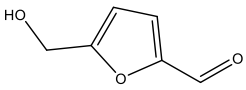
16	13.035	11.9433	4H-Pyran-4-one, 2,3-dihydro-3,5-dihydroxy-6-methyl-	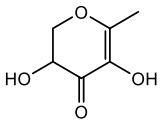
25	16.389	7.9822	1,2,3-Benzenetriol	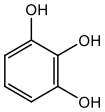
24	16.082	4.4273	3-Acetyl-2,5-dimethylthiophene	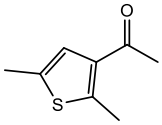
21	14.967	4.1572	Hydroquinone	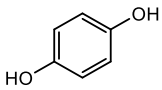
36	20.371	3.5636	Benzamide, 3,4-fluoro-	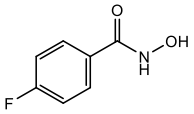
37	20.56	3.4646	2,4-Dimethylpentan-3-yl (E)-2-methylbut-2-enoate	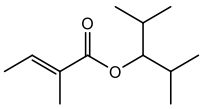
17	13.569	3.4459	.alpha.-Terpineol	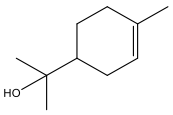
34	19.413	2.2972	Nonane, 4-methyl-5-propyl-	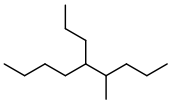
18	13.804	2.26	Catechol	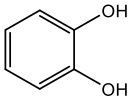
38	20.646	1.7751	Oxalic acid, isohexyl 1-menthyl ester	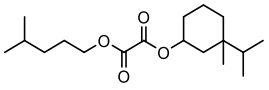
12	11.88	1.6448	Furyl hydroxymethyl ketone	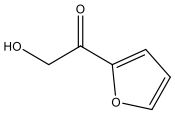
31	18.117	1.2473	Durohydroquinone	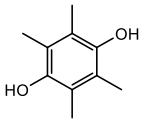
5	9.429	1.0622	2-Furancarboxaldehyde, 5-methyl-	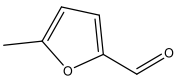

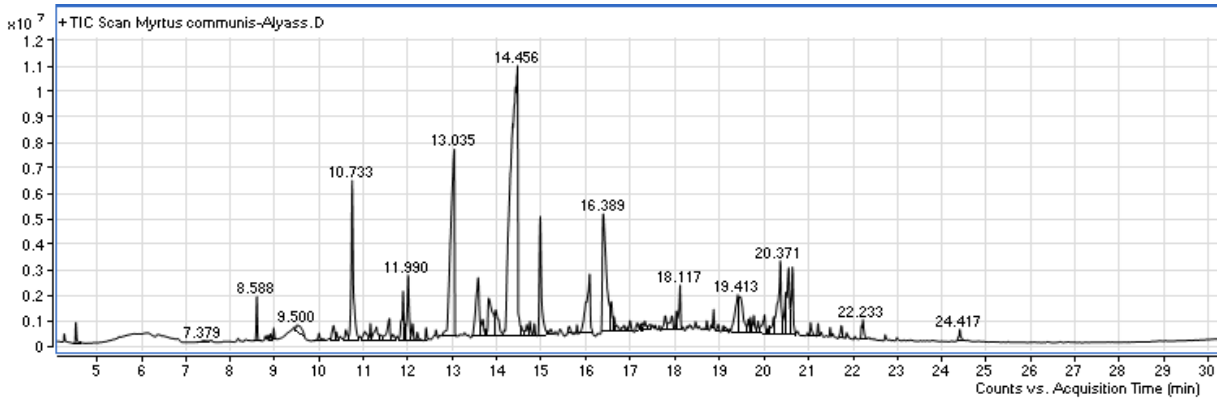

Fig. 2. *GC-MS chromatogram of the aqueous extract of Myrtus communis L.*

an increase in the sorbent's porosity and total pore volume, and an increase in the number of active sites that are available for adsorption. The results of the statistical analysis indicated significant differences between types of cellulose and the temperature at ≤0.05.

Effect of adsorbent dose

Adsorbent dose is an important parameter that strongly influences the adsorption process by affecting the adsorption capacity of the adsorbent. The effect of adsorbent dosage on adsorption for Safranine The cellulose materials were evaluated by the weight range from 0.2 to 0.6 g and a solution of 100 ppm. As shown in the (Figs.14 and 15), the highest efficiency is about 53.88% for ST and 89.56% at 0.4 g. Higher removal of dyes with increasing adsorbent dosage is attributed to the increase in total adsorbent surface area and adsorption sites. The results of the statistical analysis indicated significant differences between the three types of cellulose and the concentrations at ≤0.05.

Adsorption isotherm

The Freundlich isotherm model (Eq. 3) works well with very heterogeneous surfaces as adsorbents (Hu *et al.,* 2010), where K_F is the Freundlich constant associated with the bonding energy, n is the Freundlich constant, and q_e is the equilibrium adsorption quantity (mg/g). The adsorption reaction's energy and intensity are determined by 1/n, and advantageous adsorption is indicated by a number of n between 2 and 10.

$$lnq_e = \frac{1}{n} lnC_e + lnK_f \qquad (3)$$

In the linear Langmuir equation (Eq. 4), q_e represents the equilibrium adsorption capacity (mg/g), C_e represents the equilibrium concentration (mg/L) in solution, and q_m represents the maximum amount of adsorption (mg/g). In relation to the energy of adsorption, the adsorption equilibrium constant is known as the Langmuir constant (K_L) (Foo and Hameed, 2010).

$$\frac{C_e}{q_e} = \frac{C_e}{q_{max}} + \frac{1}{K_L q_{max}} \qquad (4)$$

Plotting the quantity sorbed qe against ln Ce allowed for the calculation of the Temkin isotherm, which is implied in Equation 5 and is characterized by a uniform distribution of binding energies (up to a certain maximum binding energy). The slope and intercept were used to calculate the constants (Chu, 2021).

$$q_e = B \ln A_T + B \ln C_e \qquad (5)$$

Where, A_T =Temkin isotherm equilibrium binding constant (L/g) and B = Constant related to heat of sorption (J/mol).

Figs. 16-18 show the adsorption isotherms of CC with saffranine dye at three temperature degrees, 25, 35, and 45 °C, using three isotherm equations, Freundlich, Langmuir, and Yemkin. Freundlich and Yemkin equations (Eq. 3 and 5), which have been successfully applied to our system and many adsorption processes,

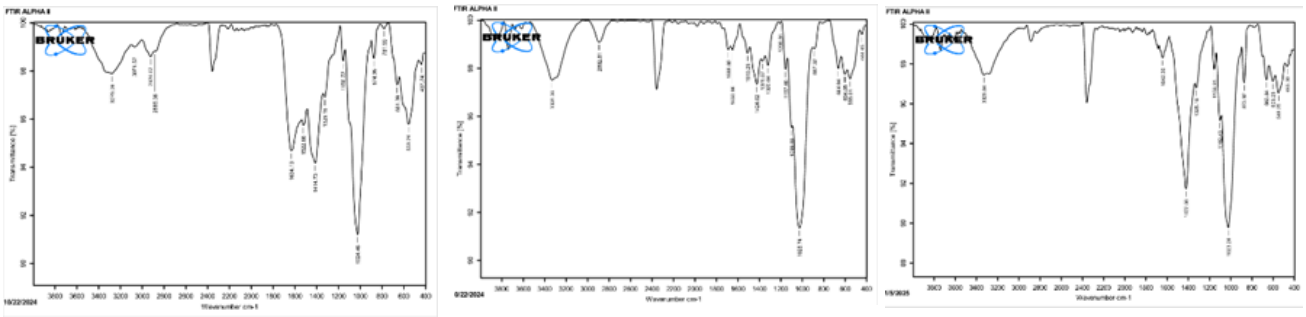

CC CAgB CAgM

Fig. 3. *FT-IR spectrum of cellulose and its composites*

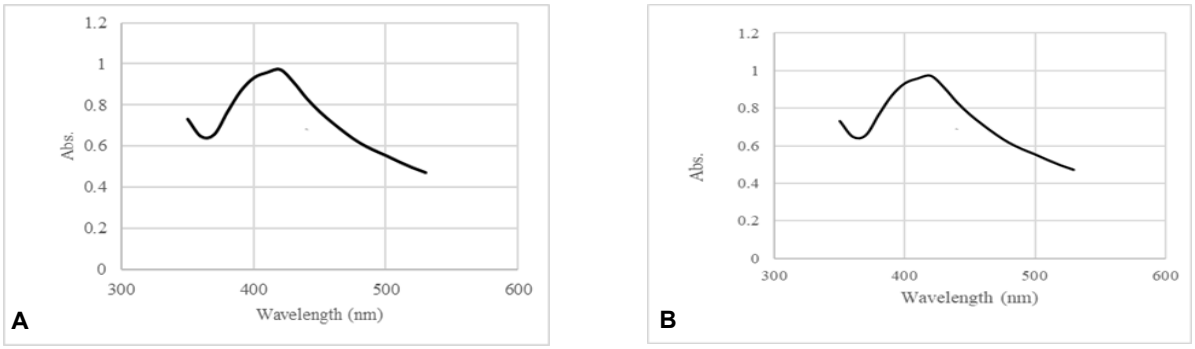

Fig. 4. *UV-vIS. spectra of AgNPs solution using A: banana peel extract, B: Myrtus communis L.* extract

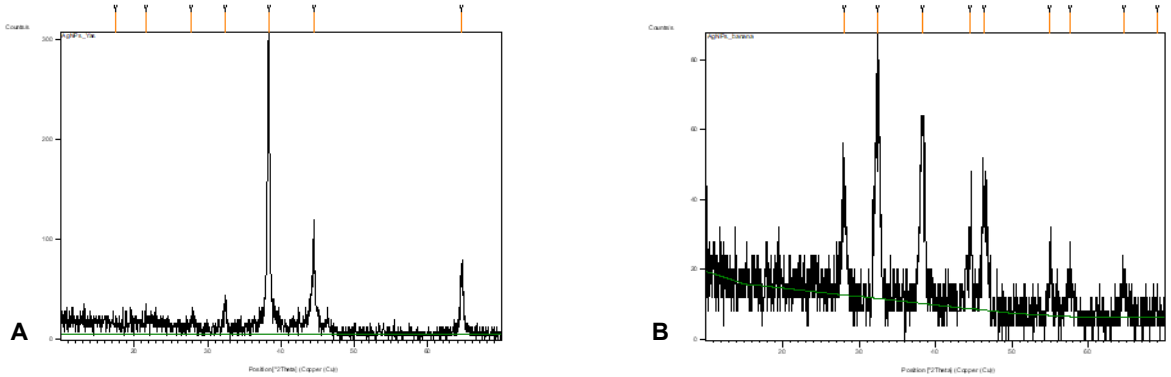

Fig. 5. *X-Ray diffraction (XRD) pattern of AgNPs using A: banana peel extract, B: Myrtus communis L.*

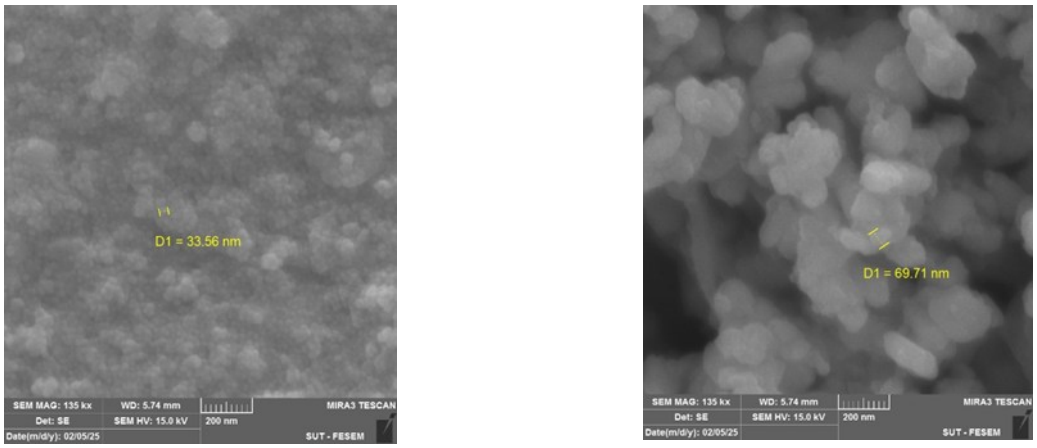

Fig. 6. *Scanning electron microscopy (SEM) of AgNPs using A: banana bells extract, B: using Myrtus communis* L.

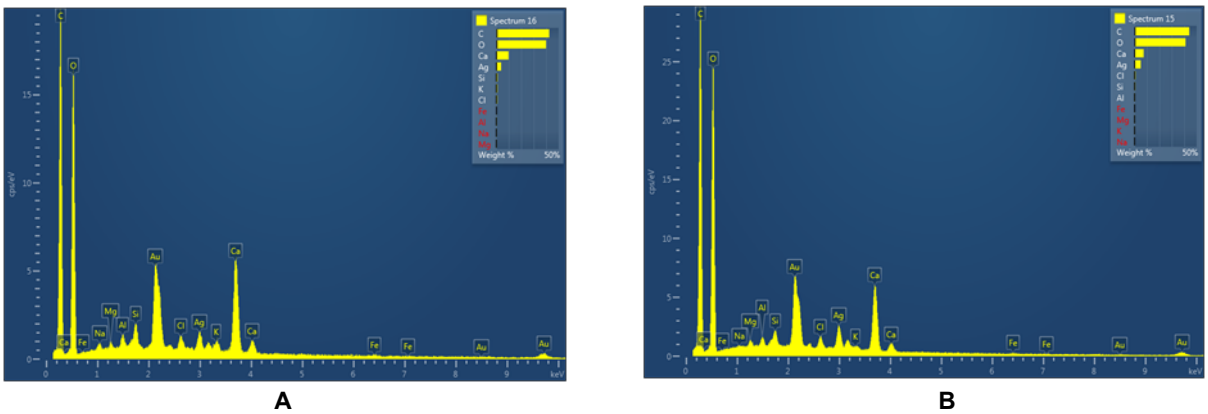

Fig. 7. *Energy dispersive X-ray spectroscopy (EDX) of A: CAgB, B: CAgM*

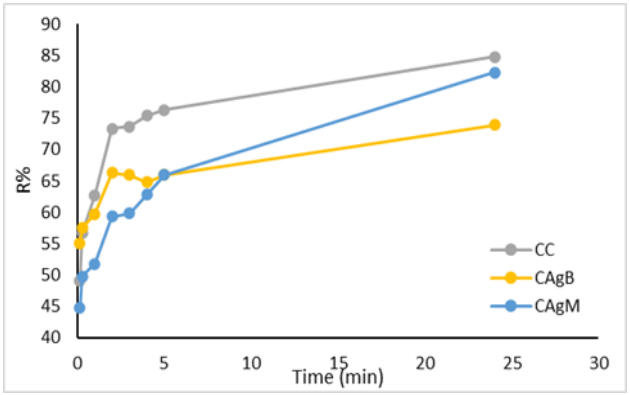

Fig. 8. *Effect of contact time on the removal efficiency (R%) of safranine T by cellulose materials*

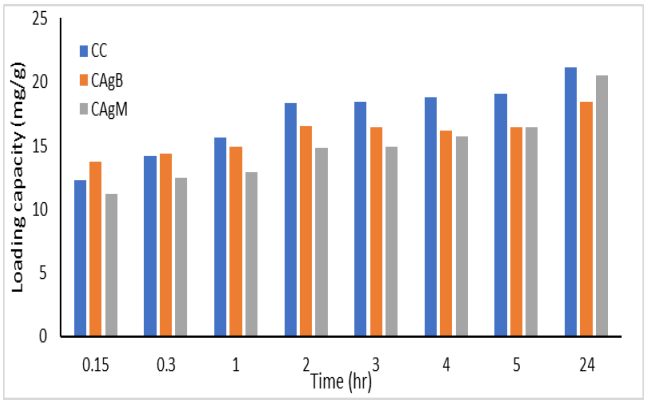

Fig. 9. *Effect of contact time on adsorption capacity (q_e) of safranine-T by cellulose materials*

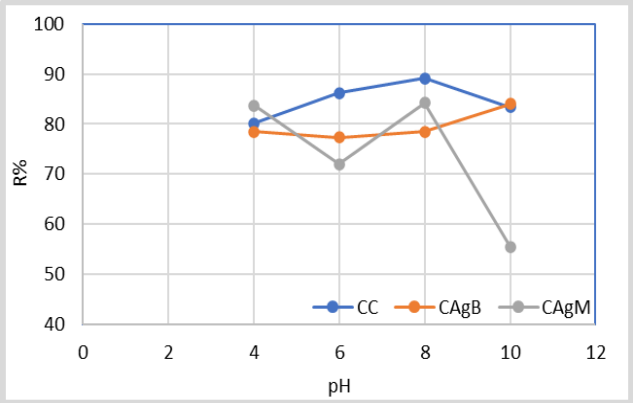

Fig. 10. *Effect of pH on the removal efficiency (R%) of safranine-T by cellulose materials*

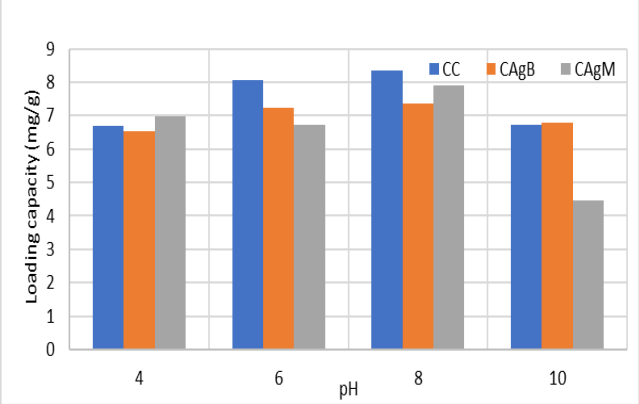

Fig. 11. *Effect of pH on the adsorption capacity (q_e) of safranine- T by cellulose materials*

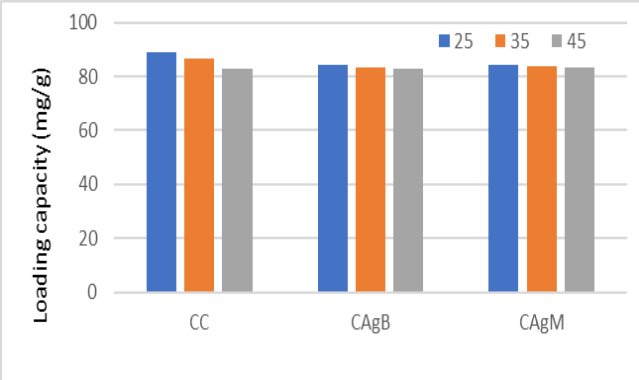

Fig. 12. *Effect of temperature on the removal efficiency (R%) of safranine by cellulose materials*

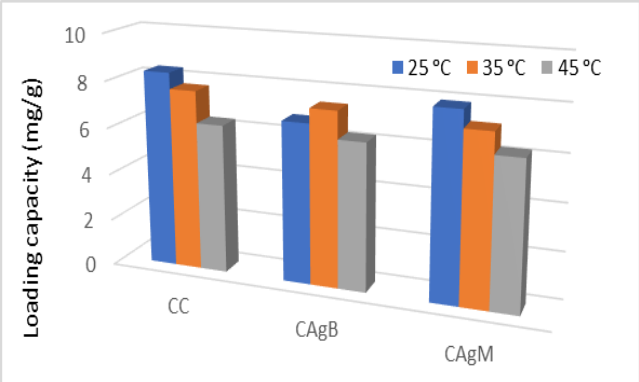

Fig. 13. *Effect of temperature on the adsorption capacity (q_e) of safranine by cellulose materials*

whereas, Langmuir equation (Eq. 4) didn't give a good correlation between the parameters.

Freundlich adsorption isotherm

This is frequently used to explain the heterogeneous surface's adsorption properties (Vigdorowitsch *et al.,* 2021). While 1/n is a function of the strength of adsorption in the adsorption process, with less than 1 denoting normal adsorption, the constant K_f is an approximation of adsorption capacity (Yaqoob *et al.*, 2022). In contrast, K_f decreased as the temperature rose, indicating that the adsorption was of the physical kind, as Table 3 and Fig. 16 demonstrate.

Langmuir adsorption isotherm

This quantitatively characterizes the development of a monolayer adsorbate on the adsorbent's exterior, following which no more adsorption occurs. The equilibrium distribution of metal ions between the solid and liquid phases is thus represented by the Langmuir (Sivaranjanee *et al.*, 2022). As illustrated in Fig. 17, the Langmuir isotherm does not provide a systematic cor-

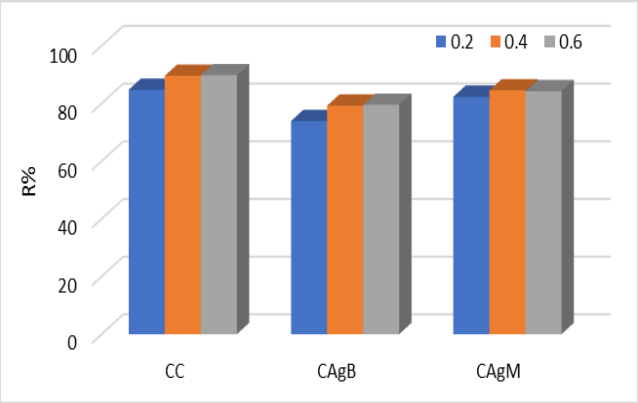

Fig. 14. *Effect of adsorbent dose on the removal efficiency (R%) of safranine by cellulose materials*

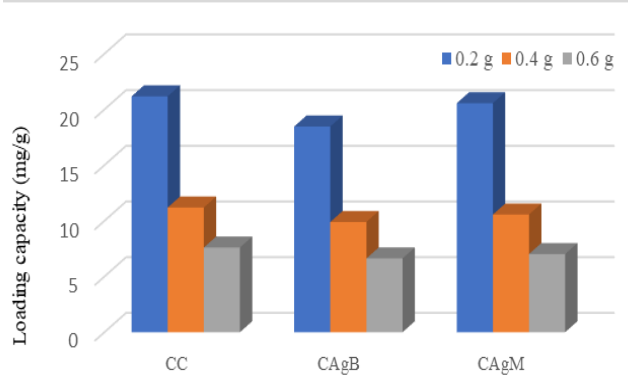

Fig. 15. *Effect of adsorbent dose on adsorption capacity (q_e) of safranine by cellulose materials*

Table 3. Constants for plotting Langmuir, Freundlich, and Temkin Adsorption Isotherms of cellulose and saffranine T dye

Temp. (°C)	Freundlich			Langmuir			Yemkin		
	1/n	K_f	R^2	q_{max}	b	R^2	B	A_T	R^2
25	0.8104	1.0874	0.9914	1.2241	9.8067	0.9328	0.5568	0.2821	0.9453
35	0.9086	0.3918	0.984	*	*	0.1606	0.5888	0.6881	0.8609
45	0.862	0.365	0.9707	*	*	0.2484	0.6096	0.7499	0.8396

*: didn't give good correlation

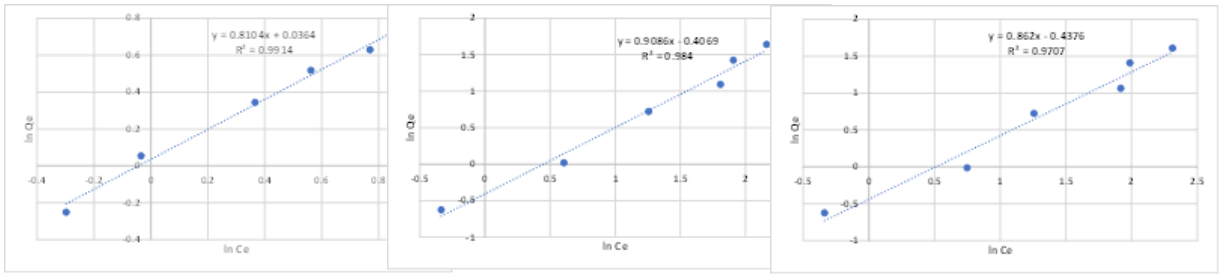

A **B** **C**

Fig. 16. *Adsorption isotherm of cellulose and saffranine T using Freundlich equation at (A) 25 °C, (B) 35 °C, and 45 °C*

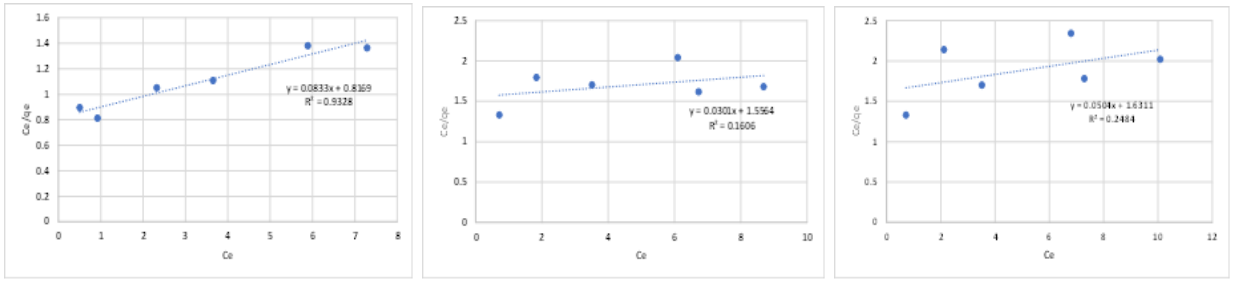

A **B** **C**

Fig. 17. *Adsorption isotherm of cellulose and saffranine T using Langmuir equation at (A) 25 °C, (B) 35 °C, and 45 °C*

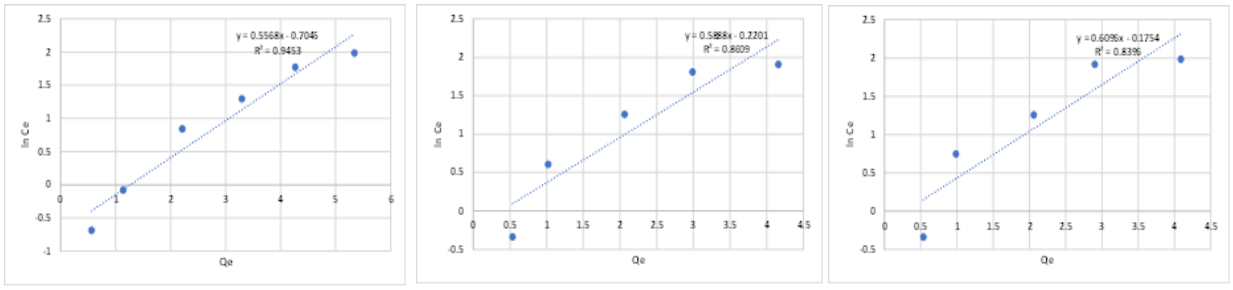

A **B** **C**

Fig. 18. *Adsorption isotherm of cellulose and saffranine T using Temkin equation at (A) 25 °C, (B) 35 °C, and 45 °C*

relation with the cellulose surface since it is only applicable to monolayer adsorption onto a flat surface with a finite number of identical sites.

Temkin adsorption isotherm

According to this isotherm, all of the molecules in the layer would have a linear drop in heat of adsorption (a function of temperature) with coverage, as opposed to a logarithmic one (Mahajan *et al.*, 2023). The average values were derived from the Temkin plot in Figure 18: average B 0.585 J/mol, which indicates the heat of sorption, showed a physical adsorption process with high correlation ($R^2 > 0.8$), and AT less than 1 indicated weak adsorption (physical adsorption).

Conclusion

In the present work, it was found that cellulose and its composites were an effective adsorbent for the removal of saffranine dye. Effect of four parameters which studied gave information that concentration of adsorbent, time of contact, pH of medium, and temperature played a main role in the adsorption process at dynamic conditions, it was found that the best adsorbent concentration is 0.4g, the adsorption process coefficient in weak alkaline media, temperature proportional inversely with adsorption removing which referred the adsorption is physical type. Statistical studies showed that there are significant differences between the three types of cellulose and the four parameters at ≤0.05. Adsorption isotherm studies showed that there was good correlation between *Ce* and q_e using Freundlich and Temkin equations, and the calculated constants showed that the type of adsorption is physical. Future research should examine the regeneration and reusability of cellulose and its composites, as well as their adsorption efficacy for a broader range of colors and pollutants, in order to determine the long-term viability of wastewater treatment applications from an economic and environmental standpoint.

Conflict of interest

The authors declare that they have no conflict of interest.

REFERENCES

1. Abu-Elghait, M., Hasanin, M., Hashem, A. H. & Salem, S. S. (2021). Ecofriendly novel synthesis of tertiary composite based on cellulose and myco-synthesized selenium nanoparticles: Characterization, antibiofilm and biocompatibility. *International Journal of Biological Macromolecules*, 175, 294–303. https://doi.org/10.1016/j.ijbiomac.2021.02.040
2. Ahankari, S., George, T., Subhedar, A. & Kar, K. K. (2020). Nanocellulose as a sustainable material for water purification. *SPE Polymers*, 1(2), 69–80. https://doi.org/10.1002/pls2.10019
3. Ahmad, M., Ahmed, E., Hong, Z., Khalid, N., Ahmed, W. & Elhissi, A. (2013). Graphene–Ag/ZnO nanocomposites as high performance photocatalysts under visible light irradiation. *Journal of Alloys and Compounds*, 577, 717–727. https://doi.org/10.1016/j.jallcom.2013.06.137
4. Alasadi, S. F., Muhammad-Ali, M. A. & Al-knaany, S. A. (2024). Using of calendula officinalis L. Plant extracts in removing some heavy metals from polluted water. *Egyptian Journal of Aquatic Biology & Fisheries*, 28 (6). http://doi.org/10.21608/ejabf.2024.391035
5. Alfarraj, N. S., Tarroum, M., Al-Qurainy, F., Nadeem, M., Khan, S., Salih, A. M., ... & Perveen, K. (2023). Biosynthesis of silver nanoparticles and exploring their potential of reducing the contamination of the in vitro culture media and inducing the callus growth of rumex nervosus explants. *Molecules*, 28(9), 3666. https://doi.org/10.3390/molecules28093666
6. Baig, N., Ihsanullah, N., Sajid, M. & Saleh, T. A. (2019). Graphene-based adsorbents for the removal of toxic organic pollutants: A review. *Journal of Environmental Management*, 244, 370–382. https://doi.org/10.1016/j.jenvman.2019.05.047
7. Bayuo, J., Rwiza, M. J., Mtei, K. M. & Choi, J. W. (2024). Adsorptive removal of heavy metals from wastewater using low-cost adsorbents derived from agro-based materials. In *Earth and Environmental Sciences Library,* (pp. 237–271). https://doi.org/10.1007/978-3-031-53688-5_11
8. Chen, J., Wang, J., Zhang, X. & Jin, Y. (2007). Microwave-assisted green synthesis of silver nanoparticles by carboxymethyl cellulose sodium and silver nitrate. *Materials Chemistry and Physics*, 108(2–3), 421–424. https://doi.org/10.1016/j.matchemphys.2007.10.019
9. Chu, K. H. (2021). Revisiting the Temkin isotherm: dimensional inconsistency and approximate forms. *Industrial & Engineering Chemistry Research*, 60(35), 13140-13147. https://doi.org/10.1021/acs.iecr.1c01788
10. Daish, M. K., Muhammad-Ali, M. A.& Al-Asadi, W. M. T. (2024, July). Green synthesis of nanoparticles using aqueous leaves extract of capparis spinosa L. and evaluation of their resistance to salt stress of some aquatic plants. In *IOP Conference Series: Earth and Environmental Science,* (1371, 2, p. 022003). IOP Publishing. http://doi.org/10.1088/1755-1315/1371/2/022003
11. Dhaka, A., Mali, S. C., Sharma, S. & Trivedi, R. (2023). A review on biological synthesis of silver nanoparticles and their potential applications. *Results in Chemistry*, 6, 101108. https://doi.org/10.1016/j.rechem.2023.101108
12. Fernandez, A., Picouet, P. & Lloret, E. (2010). Reduction of the spoilage-related microflora in absorbent pads by silver nanotechnology during modified atmosphere packaging of beef meat. *Journal of Food Protection*, 73(12), 2263–2269. https://doi.org/10.4315/0362-028x-73.12.2263
13. Foo, K. Y. & Hameed, B. H. (2010). Insights into the modeling of adsorption isotherm systems. *Chemical Engineering Journal*, 156(1), 2-10. https://doi.org/10.1016/j.cej.2009.09.013
14. Hu, Z., Chen, H., Ji, F. & Yuan, S. (2010). Removal of congo red from aqueous solution by cattail root. *Journal of Hazardous Materials*, 173(1-3), 292-297. https://doi.org/10.1016/j.jhazmat.2009.08.082
15. Islam, M. T., Jing, H., Yang, T., Zubia, E., Goos, A. G., Bernal, R. A., Botez, C. E., Narayan, M., Chan, C. K. & Noveron, J. C. (2018a). Fullerene stabilized gold nanoparticles supported on titanium dioxide for enhanced photocatalytic degradation of methyl orange and catalytic reduc-

tion of 4-nitrophenol. *Journal of Environmental Chemical Engineering*, 6(4), 3827–3836. https://doi.org/10.1016/j.jece.2018.05.032

16. Islam, M. T., Jing, H., Yang, T., Zubia, E., Goos, A. G., Bernal, R. A., Botez, C. E., Narayan, M., Chan, C. K. & Noveron, J. C. (2018b). Fullerene stabilized gold nanoparticles supported on titanium dioxide for enhanced photocatalytic degradation of methyl orange and catalytic reduction of 4-nitrophenol. *Journal of Environmental Chemical Engineering*, 6(4), 3827–3836. https://doi.org/10.1016/j.jece.2018.05.032
17. Jasim, E. Q., Muhammad-Ali, M. A. & Al-Abdullah, A. A. (2024). In vitro studies of biosynthesized nanoparticles of dysphania aqueous leaves extract against some isolated bacteria from wounds and burns and in silico evaluations of compounds identified in its GC-MS Spectra. *Tropical Journal of Natural Product Research*, 8(11). https://doi.org/10.26538/tjnpr/v8i11.26
18. Jóźwiak, T., Filipkowska, U., Bednarowicz, A., Zielińska, D. & Wiśniewska-Wrona, M. (2024). The use of various types of waste paper for the removal of anionic and cationic dyes from aqueous solutions. *Molecules*, 29(12), 2809. https://doi.org/10.3390/molecules29122809
19. Kara, H. T., Anshebo, S. T., Sabir, F. K. & Workineh, G. A. (2021). Removal of methylene blue dye from wastewater using periodiated modified nanocellulose. *International Journal of Chemical Engineering*, 2021, 1–16. https://doi.org/10.1155/2021/9965452
20. Mahajan, T., Paikaray, S. & Mahajan, P. (2023, October). Applicability of the equilibrium adsorption isotherms and the statistical tools on to them: a case study for the adsorption of fluoride onto Mg-Fe-CO3 LDH. In *Journal of Physics: Conference Series,* (2603, No. 1, p. 012056). IOP Publishing. https://doi.org/10.1088/1742-6596/2603/1/012056
21. Mishra, K., Siwal, S. S., Sithole, T., Singh, N., Hart, P. & Thakur, V. K. (2024). Biorenewable materials for water remediation: the central role of cellulose in achieving sustainability. *Journal of Bioresources and Bioproducts*, 9(3), 253-282. https://doi.org/10.1016/j.jobab.2023.12.002
22. Nadagouda, M. N. & Varma, R. S. (2007). Synthesis of thermally stable carboxymethyl cellulose/metal biodegradable nanocomposites for potential biological applications. *Biomacromolecules*, 8(9), 2762–2767. https://doi.org/10.1021/bm700446p
23. Padilla, J. E., Melendez, J., Barrera, L. A., Wu, Y., Ventura, K., Veleta, J. M., Islam, M. T., Chavez, C. A., Katla, S. K., Villagrán, D.& Noveron, J. C. (2017). High dispersions of carbon nanotubes on cotton-cellulose benzoate fibers with enhanced electrochemical generation of reactive oxygen species in water. *Journal of Environmental Chemical Engineering*, 6(1), 1027–1032. https://doi.org/10.1016/j.jece.2017.12.002
24. Rasli, S. R. (2017). Extraction and characterization of cellulose from agricultural residue - oil palm fronds. *Malaysian Journal of Analytical Sciences*, 1065-1073. https://doi.org/10.17576/mjas-2017-2105-08
25. Ritter, M. T., Lobo-Recio, M. A., Padilla, I., Nagel-Hassemer, M. E., Romero, M. & López-Delgado, A. (2024). Adsorption of safranine-T dye using a waste-based zeolite: Optimization, kinetic and isothermal study. *Journal of Industrial and Engineering Chemistry*, 136, 177-187. https://doi.org/10.1016/j.jiec.2024.02.005
26. Saha, S., Shukla, S. K., Singh, H. R., Pradhan, K. K. & Jha, S. K. (2020). Production and purification of bioflocculants from newly isolated bacterial species: a comparative decolourization study of cationic and anionic textile dyes. *Environmental Technology*, 42(23), 3663–3674. https://doi.org/10.1080/09593330.2020.1737737
27. Salman, H. H., Ali, M. A. M. & Ali, E. T. (2020). Synthesis and screening of anticancer potentials of some new terephthaldehyde-derived nitrone compounds. *Tropical Journal of Pharmaceutical Research*, 19(2), 341-349. https://doi.org/10.4314/tjpr.v19i2.17
28. Sedighi, A., Montazer, M. & Samadi, N. (2014). Synthesis of nano Cu2O on cotton: Morphological, physical, biological and optical sensing characterizations. *Carbohydrate Polymers*, 110, 489–498. https://doi.org/10.1016/j.carbpol.2014.04.030
29. Sivaranjanee, R., Kumar, P. S. & Mahalaxmi, S. (2022). A review on agro-based materials on the separation of environmental pollutants from water system. *Chemical Engineering Research and Design*, 181, 423-457. https://doi.org/10.1016/j.cherd.2022.04.002
30. Štular, D., Savio, E., Simončič, B., Šobak, M., Jerman, I., Poljanšek, I., ... & Tomšič, B. (2021). Multifunctional antibacterial and ultraviolet protective cotton cellulose developed by in situ biosynthesis of silver nanoparticles into a polysiloxane matrix mediated by sumac leaf extract. *Applied Surface Science*, 563, 150361. https://doi.org/10.1016/j.apsusc.2021.150361
31. Suleman, M., Zafar, M., Ahmed, A., Rashid, M. U., Hussain, S., Razzaq, A., Mohidem, N. A., Fazal, T., Haider, B. & Park, Y. (2021). Castor leaves-based biochar for adsorption of safranin from textile wastewater. *Sustainability*, 13(12), 6926. https://doi.org/10.3390/su13126926
32. Tomar, R. S. & Preet, S. (2017). Evaluation of anthelmintic activity of biologically synthesized silver nanoparticles against the gastrointestinal nematode, Haemonchus contortus. *Journal of Helminthology*, 91(4), 454-461. https://doi.org/10.1017/S0022149X16000444
33. Vigdorowitsch, M., Pchelintsev, A., Tsygankova, L. & Tanygina, E. (2021). Freundlich isotherm: An adsorption model complete framework. *Applied Sciences*, 11(17), 8078. https://doi.org/10.3390/app11178078
34. Walawska, A., Olak-Kucharczyk, M., Kaczmarek, A. & Kudzin, M. H. (2024). Environmentally friendly bleaching process of the cellulose fibres materials using ozone and hydrogen peroxide in the gas phase. *Materials*, 17(6), 1355.
35. Yaqoob, G. B. (2022). Adsorption of some heavy elements on surface of activated carbonized cellulose from aqueous solution. *Journal of Petroleum Research and Studies*, 12(2), 110-122. http://doi.org/10.52716/jprs.v12i2.661